

Optimization of Spinning Disk Confocal Microscopy: Synchronization with the Ultra-Sensitive EMCCD

F. K. Chong^a, Colin G. Coates^a, Donal J. Denvir^a, Noel McHale^b, Keith Thornbury^b and Mark Hollywood^b.

^aAndor Technology Ltd., 9 Millennium Way, Springvale Business Park, Belfast, BT12 7AL. Tel. +44 (0)28 90237126;

^bSmooth Muscle Group, Medical Biology Centre, Queen's University of Belfast, Belfast BT9 7BL.

ABSTRACT

The advent of Electron Multiplying Charge Coupled Device (EMCCD) technology and its ability to overcome previous hurdles in low-light fluorescence microscopy, such as phototoxicity to live cells, photobleaching of fluorophores and exposure time restrictions, has resulted in a significant resurgence of interest in use of confocal spinning disk techniques for live cell microscopy. Here provide an understanding of, and technical solutions to, the issues of synchronization that have previously marred the coupling of fast CCD camera technology to confocal spinning disk arrangements. We examine the challenges arising from both old and new models of the Nipkow spinning disk confocal unit and suggest solutions throughout based on a sound comprehension of both (a) relative scan/exposure times; (b) relative orientation of the coupled devices; (c) optimisation of EMCCD clocking parameters.

Keywords: CCD, EMCCD, Nipkow, Confocal spinning Disk, Confocal Microscopy, Live Cell Microscopy, Electron Multiplying CCD, Single Photon Sensitivity.

1. INTRODUCTION

Electron Multiplying Charge Coupled Device (EMCCD) camera technology is having a profound influence on the field of low-light dynamic microscopy, combining highest possible photon collection efficiency with the ability to virtually eliminate the readout noise detection limit. The EMCCD is an advanced CCD camera design, offering unsurpassed sensitivity performance, and has been shown to yield markedly improved S/N under ultra low-light conditions *at high speed operation*, uniquely facilitating the demanding fast speed low-light microscopies such as single molecule detection, intracellular ion signalling microscopy and 4D live cell microscopy. The detector makes use of a new CCD architecture¹⁻⁵ that unites the single photon sensitivity of an ICCD, with the inherent Quantum Efficiency (QE up to 95%), pixel resolution advantages and durability of a CCD.

Such on-chip amplifying sensor technology is sold by both E2V and Texas Instruments (TI) under the trade names 'L3Vision' and 'Impactron', respectively. Presently four EMCCD scientific digital camera formats are commercially available from Andor under the part numbers DV860, DV865, DV887 and DV885, with sensor formats ranging from 1000x1000 to 128x128 pixels, the latter delivering up to 500 full frames/sec. Both front and back-illuminated versions of the DV860 and DV887, with 128x128 and 512x512 pixel formats respectively, have been evaluated previously in terms of sensitivity, signal to noise ratio (S/N), resolution, and the significant performance benefits over say Gen III+ Intensified CCDs (ICCDs) have been thoroughly substantiated.³⁻⁵

Techniques such as intracellular ion signalling and single molecule microscopy have been restricted in the past by severe limitations in both instrument sensitivity and speed – the parameters that EMCCD technology has been designed to directly address. Sensitivity is critical to: (i) detect the weak signal of low dye concentrations; (ii) cope with the lower photon fluxes afforded by shorter exposure times (complementing fast frame rates); (iii) detect the weaker photon fluxes afforded by reduced excitation powers (reducing photobleaching of dyes and phototoxicity to tissues, thereby lengthening experimental lifetimes); (iv) overcome the significant readout noise detection limit of high speed readout rate. High frame rates are required to facilitate the direct imaging of rapid intracellular events over multiple dimensions, enabling for example, rapid 3D volume reconstructions of live cells, resolved over both time and wavelength. The ability

to carry this out with markedly lower excitation powers means that the live cells can be visualized over much longer kinetic series.

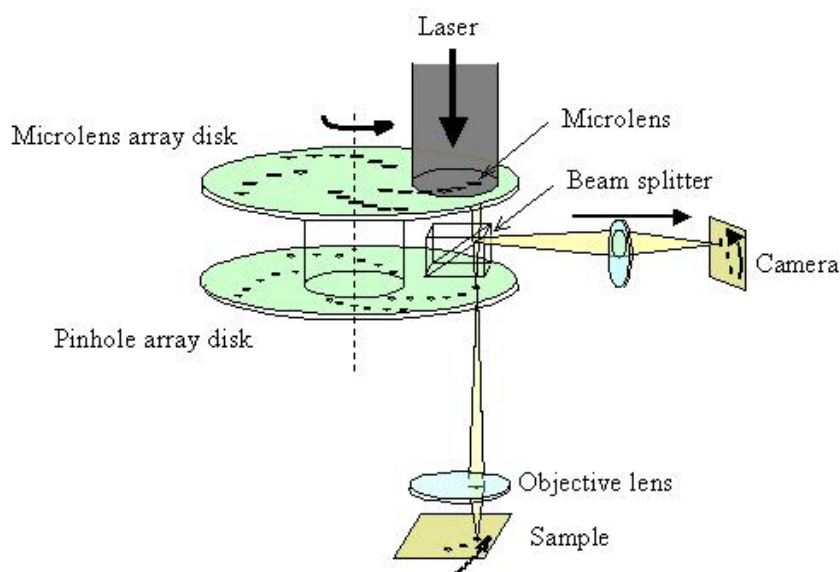
Of particular significance to intracellular microscopy, the most recent addition to the EMCCD range is the 1Kx1K DV885 camera, containing the first such sensor to successfully combine this technology with smaller pixels, suited to resolving resolution of fine intracellular detail. While ideal in terms of pixel size, one must always remember that smaller $8 \times 8 \mu\text{m}$ pixels result in lower S/N since less photons are collected within the smaller pixel areas. Furthermore, this sensor does not yet exist in back-illuminated format, using instead a technology called 'virtual phase' that does yield higher QE than traditional front-illuminated sensors, particularly at blue wavelengths (in terms of QE performance virtual phase can be considered as a hybrid of front and back-illuminated sensors). If the absolute QE performance of a back-illuminated sensor is deemed necessary, yet fine resolution of intracellular structure is still desirable, a back-illuminated 512x512 DV887 sensor with $16 \times 16 \mu\text{m}$ can be used in conjunction with a c-mount lens to magnify the image further before the sensor (thereby effectively reducing pixel sizes). Caution is needed here to ensure that the CCD makes use of a solid hermetic vacuum seal and that only one window exists in front of the sensor. Use of such a coupling lens with a two or more window CCD design (as is used for example in o-ring sealed CCD cameras) results in image curvature - not to mention the photon reflection of the extra non anti-reflection coated window.

The Nipkow spinning disk was designed in 1884 by German inventor Paul Nipkow as a way to transmit images electrically using a pair of spinning metal disks. He punched holes in a spiral pattern along these disks, one of which was housed in a transmitter and the other in a receiver. The first disk scanned an object as light shone through its holes onto selenium, changing the electrical current, causing a lamp in the receiver to flicker. Anyone looking at the lamp through the second spinning disk saw the original image revealed. This development led to the first demonstration of television in 1926. Approximately 50 years later the Nipkow disk began to be adapted for rapid confocal scanning in microscopy, with the clear speed advantage over conventional confocal point scanning. This scan rate advantage has clear benefits with regard to following rapid intracellular dynamics and also recording confocal stacks for 4D live cell reconstruction.

Yokogawa Electric Corporation have optimised the Nipkow confocal scanning in the CSU units through use of a second spinning disk containing 20,000 microlenses,^{8,9} each one coupled to one of the pinholes of the second disk, as illustrated in the diagram below. This approach has improved transmission efficiency in the system from 1% to nearly 70%. The original CSU10 Yokogawa system operates at a fixed disk speed of 1800 rev/min, yielding a reported possible 360 full raster scanned confocal images per second. In fluorescence confocal microscopy, at any one time an input laser illuminates approximately 1000 of the microlenses, focusing the light through the same number of pinholes, and the multiple 'minibeams' are focused by the objective onto the focal plane. As the disk rotates, each beam scans across a portion of the focal plane, with the result that every point of the field of view is scanned within a very short time. Emitted fluorescence from each scanned point is collected by the same objective and focused through the pinhole onto a dichroic mirror and onto the respective pixels of the CCD to build up the image. Until recently, the Nipkow unit has almost invariably been used at a faster sample rate than the frame rate capabilities of the CCD. Now however, EMCCD cameras exist that can deliver up to 500 full frames/sec, and provide the raw sensitivity to detect the reduced number of photons that accompany such short camera exposures, especially from such an inherently low-light technique. A highly significant benefit of the Nipkow confocal disk approach relates to its suitability to live cell fluorescence microscopy, in that it has been determined to inflict markedly reduced photodamage to the cells in comparison to confocal point scanning approaches. This is due to the use of $1/1000^{\text{th}}$ of excitation peak power that is routinely employed in conventional point scanning. Thus, live cell samples can be imaged for longer periods of time, without risk of phototoxic degradation.

Whilst the spinning disk confocal microscope is in concept highly applicable to use for multi-dimensional live cell microscopy and intracellular ion signalling microscopy etc., it nevertheless remains a confocal technique and is therefore inherently low-light in nature. This attribute has imposed limitations in terms of the minimum acceptable laser power, camera exposure time and fluorophore concentrations required to yield images of acceptable S/N quality, which in turn have restricted maximum time of live cell scanning, frame rates and the ability to minimize effects such as Ca^{2+} buffering in intracellular studies.^{6,7} These factors combined have until recently marred the take-up of confocal spinning disk as a completely revolutionary technology for live cell imaging.

The launch of the EMCCD range has resulted in a significant awakening with regard to this method, and indeed, we have produced recent publications that show how the considerable sensitivity and speed boost of this technology can be used to optimise this promising live cell approach.³



Diagrammatic representation of the Yokogawa Nipkow spinning disk technology

However, spinning disk technology has been restricted by some further factors, namely the image artefacts that can arise as a result of non-synchronisation of the spinning disk with the CCD camera exposures. This has been widely observed to result in banding patterns superimposed onto the image that can limit image quality. Such banding patterns have been more prominent when short CCD exposure times are used, since under these conditions, the partially scanned Nipkow image would represent a greater proportion of the total CCD exposure. Since many dynamic processes require rapid frame rates, this is a very common problem.

Here we examine the banding effects in more detail and provide an understanding of the underlying causes, and also propose solutions. We make use of spinning disk systems from Yokogawa Electric Corporation to examine these effects, both the CSU10 and CSU22 models. Many CSU10 models exist in laboratories around the world, and the reported synchronisation difficulties with sensitive CCD cameras and banding problems have been widespread. At the time of writing the CSU22 model is just emerging onto the market. One fundamental difference between these models is in the ability to vary the disk rotation speed in the CSU22, whereas the spin rate is fixed at a steady 1800 rpm in the CSU10. The ability to vary the disk speed should make synchronisation to the CCD more realisable. Here we provide a more detailed understanding of the CCD coupling challenges of both spinning disk models and also provide and experimentally validate effective synchronisation solutions for each.

2. EXPERIMENTAL

EMCCD Cameras

The iXon DV887 (BV) from Andor Technology is a 10 MHz camera with a 512x512 frame-transfer sensor, 16 μm^2 pixel size, capable of delivering >30 full frames/sec (the precise value dependent on the vertical row shift speed selectable through the software). It is important to note that much faster frame rates still are achievable through selection of sub-arrays and/or binning. Some frame rates resulting from pixel binning and sub-array combinations are given in Table 1 below, assuming a 0.4 μs /row vertical shift speed. It is particularly interesting to note that 169 frames/sec is available through 100x512 sub array, without any resolution sacrifice of pixel binning. This shape of active CCD area corresponds (using a x100 objective) to a field of view of 16 μm x 82 μm that is sufficient to image a large proportion of a typical

smooth muscle cell. Recording in this mode enables such cells to be imaged at very high temporal and spatial resolution. Furthermore, the superior camera sensitivity is such that the S/N advantages associated with pixel binning may readily be sacrificed in favour of maintaining resolution.

<i>Array size/Binning</i>	<i>512x512 (full frame)</i>	<i>256x256</i>	<i>128x128</i>	<i>100v x 512h</i>
1x1	35.5	70	135	169
2x1	69	133	250	312
2x2	69	133	250	312
4x1	131	244	435	526
4x4	131	244	435	526

Table 1 –Frame rates (frames per second) achievable from the back-illuminated 10 MHz Andor iXon DV887 at a variety of sub-array and binning combinations.

Basic Nipkow Synchronisation Visualisation

An inverted Nikon TE2000 Microscope with x20 objective was combined, in turn, with both CSU10 and CSU22 Nipkow confocal disk units (Yokogawa Electric Corporation, Japan). A segment of grey printed paper was fixed onto the stage and imaged by transmission microscopy, images of black ink granules were easily obtained, the region between the granules providing a clear area of light transmission. For many of the synchronisation measurements, the image was purposefully defocused since the banding patterns are more observable against a more diffuse background.

Intracellular Ion Measurements

An inverted Nikon TE300 Microscope with x40 and x100 objectives was combined with the CSU10 spinning Nipkow disk unit and a Krypton/Argon Ion laser with excitation wavelength 488 nm. Freshly dispersed rabbit urethral and guinea-pig cells were obtained as described previously^{6,7} and were loaded with 10 μ M of Fluo-4-AM dye (Molecular Probes, emission maximum at 516 nm) for 15 minutes at 37°C. When bound to free Ca²⁺, the emission quantum yield of Fluo-4 increases significantly. Caffeine addition (10 mM for 5 seconds) was used to induce release of intracellular Ca²⁺ from the cellular calcium stores and resulted in a rapid build up (over 10's milliseconds) of Ca²⁺ levels within the cell, followed by a slower (100's milliseconds – seconds) decay of the intracellular Ca²⁺ concentration.

3. RESULTS AND DISCUSSION

In this section we will show how, upon closer examination, the banding patterns can be separated into two sources: (i) one pattern appears as a result of the directional shifting of the charge under the mask of the frame transfer CCD (during readout) relative to the direction of the pinhole movement on the disk; (ii) the other banding pattern arises from non-synchronisation of a whole number of disk scans within a single exposure of the CCD.

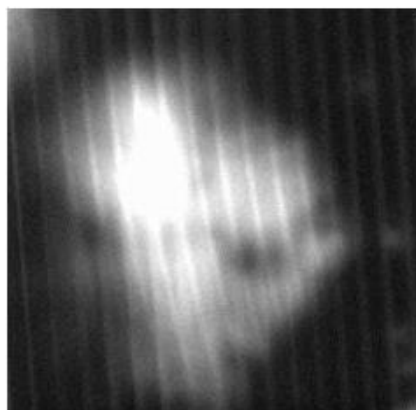
In the present experiments we made use of brightfield microscopy images of ink granules on printed paper, using a x20 objective, as a simple means to observe these banding patterns. We had noted that the pattern is more apparent if the object is made more diffuse, so the image of the granule was defocused slightly. Figure 1 shows a representative image that is uncorrected for either of the banding effects. In order to demonstrate these artefacts separately, we eliminated one effect to leave the other effect exposed, such that the respective methods for elimination can be visualized more readily.

A – Frame Transfer Effect

We will deal first with the frame transfer effect, an effect that should be identically treatable for both CSU10 and CSU22 versions of the Nipkow confocal unit. This effect results in line patterns, extending more notably from brighter regions of the Nipkow image into background region of the image.

In order to ensure that we were observing only the pattern due to the frame transfer effect, we took steps to eliminate the patterns that may arise from synchronisation effects, as described more fully later.

Figure 2 shows a selected series of images taken as the camera was rotated slowly relative to the Nipkow unit. It is important to note that the images were taken using a $6.6 \mu\text{s}/\text{row}$ vertical (or parallel) shift time, referring to the time taken to shift 1 row of pixels down towards the masked CCD area during the readout process. This shift time corresponds to that which is typical of the ability of the majority of such cameras on the market. It is apparent that during rotation, the camera passes through a region where the frame shift banding pattern is minimized. It is also apparent that the lines observed move from a horizontal orientation, pass through a 'clean' area and then reappear quite strongly in a more vertical orientation. The effect arises from an interaction between the moving holes of the Nipkow disk and the Frame Transfer CCD. In any FT CCD the image is integrated on the image area but then it must be moved down into the storage area to be readout, this transfer time is usually short compared to the integration time but still results in a small



Overlap of two banding effects

Figure 1 – Representative unsynchronised image.

amount of image smear. This is nothing new for FT CCDs. In this instance however, because our image is not stationary but being made up from a series of scanning pinholes, there will be some kind of beating effect between the moving image and the moving holes. It is not possible to do a full analysis here but it should be obvious that the effect will be dependent on the speed and direction of the spinning disk relative to the speed and direction of the moving image.

A more effective solution to the frame transfer artefact has been realised however, through pushing the vertical shift times to shorter values. This is an ability that is exclusive to Andor's iXon range and has arisen through extensive R&D attention given to clocking parameters. For example, Andor offer the ability in software for the user to select different clocking voltages that enable very short vertical shift times to be employed without suffering charge lag effects (i.e. leaving a percentage of the charge behind) which would otherwise result in serious image distortions.

Figure 3 (a) shows defocused granule images taken at a CCD orientation that, at $6.6 \mu\text{s}/\text{row}$ vertical shift time, exhibits quite severe frame transfer banding patterns. However, the iXon is capable of pushing to significantly shorter values and it is clear that the images taken using 1.8 and $0.6 \mu\text{s}/\text{row}$ show a marked improvement in this effect. In fact, at $0.6 \mu\text{s}/\text{row}$, the frame shift banding has been effectively eliminated. Figure 3 (b) shows a further set of images for which it is clear that the effect seems to have been virtually eliminated even at $1.8 \mu\text{s}/\text{row}$. Figure 3(c) shows some granules brought more into focus to verify that the effect can still be observed under these conditions. Again, it is clear that the banding lessens with faster vertical shifts and appears to be eliminated by $1.8 \mu\text{s}/\text{row}$.

B- Synchronisation of the CSU22

The Yokogawa CSU22 Nipkow confocal unit is a more advanced design than its predecessor, the CSU10, in that it is not only capable of faster spin rates (up to 5000 rev/min) but it is entirely tuneable up to this speed. This design means that in theory a disk speed can be selected that yields a confocal scan time that is either exactly matched to or divisible by a whole number into the exposure time of the CCD camera.

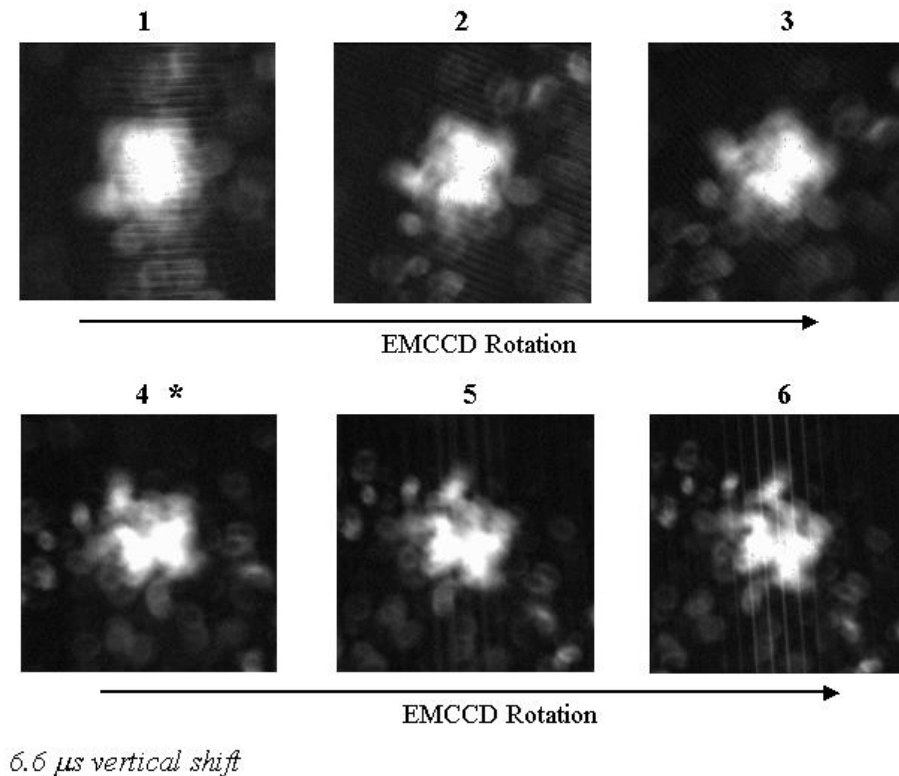


Figure 2 – Effect of camera orientation relative to the Nipkow unit on the frame shift banding effect, employing a $6.6 \mu\text{s}/\text{row}$ vertical shift time. The fourth image in the series shows the optimal orientation.

This ‘exposure matching’ is important since a partial confocal image within the exposure time of the CCD will again result in a banding effect superimposed over the entire image area (of a distinct origin than that generated by the aforementioned frame transfer effect). This is a key point in that one must be very careful when synchronising the two, that it is the relative exposure time and not frame rate that is considered. This is because the frame rate of a frame transfer CCD must also take into account some other readout overheads such as the time to shift the image under the mask, i.e. the cycle time will be slightly longer than the exposure time. So, one should not determine the image rate of the Nipkow disk at a certain disk speed and make it divisible into the camera frame rate. Instead one should determine the time it takes for the Nipkow disk to perform a complete image scan at that disk speed and make it divisible into the camera exposure time. The advantage of a tunable disk speed is that this can be accomplished for any given camera exposure time.

It is also necessary to consider the temporal alignment of the camera and Nipkow unit, since one might imagine that an external pulse must be fed into the two in order that the beginning of a camera exposure corresponds exactly to the beginning of a Nipkow scan. However, the situation is in fact made much simpler than this by virtue of the Nipkow design. The CSU units contain a Nipkow disk containing 20,000 pinholes arranged in an archimedes spiral, this disk coupled to an identical spinning disk of 20,000 microlenses. The layout of the pinholes and microlenses is such that on each full revolution of the spinning disk, twelve complete images have been confocally scanned. That is to say, the disk can be thought of as split into twelve identical segments, each one resulting in a full image scan. The crucial point to accept is that these segments do not have defined start and end points on the disk, i.e. as the disk is spinning and we took a CCD exposure corresponding to one twelfth of a disk rotation, a fully scanned image will have been projected onto the CCD sensor, irrespective of at what point in the revolution the exposure was started. This actually makes the situation much less complicated (and costly) since the CCD and Nipkow unit can be run internally, and do not need to be synched by external pulses. All one needs to be concerned with is that the number of full Nipkow scans is wholly divisible into the CCD exposure time. We also must be sure that the timing parameters in both CCD and Nipkow unit are totally

accurate and entirely stable. Since both the camera and the disk use crystal oscillators for their timing, this accuracy is achieved.

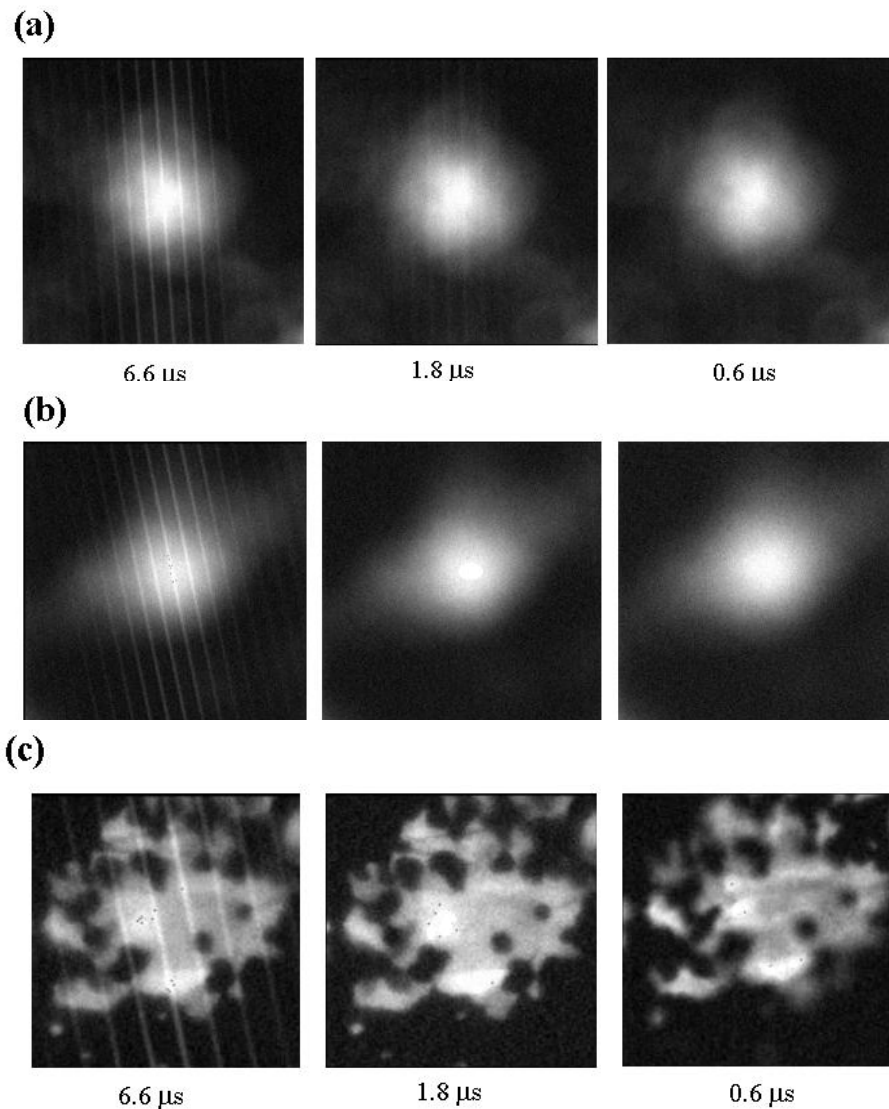


Figure 3 – Effect of EMCCD vertical shift time on frame shift banding effect at fixed unoptimised camera orientation.

To illustrate this concept, Figure 4 shows a montage of defocused granule images taken from a 500 frame kinetic series of images, recording the spinning disk as it slows down from 5000 rev/min to 1800 revs/min. In order to observe only the synchronization effect, measures were taken to eliminate the frame shift pattern, as described above. The exposure time of the CCD employed was 19.44 ms, which corresponds to the time taken for 7 Nipkow full disk scans at the 1800 rev/min speed (12 segments at 360 segments per second). A faint diagonal banding pattern is observed across the image in the initial frames. As the disk slows further it enters a region (frame 29) where the banding disappears. This corresponds to a disk speed that yields a scan time that is divisible into the CCD exposure time. It goes through several more such synchronisation cycles before settling at 1800 rev/min in the final frames where, as expected, the banding is not present. Frames 2, 77, 310 and 332 represent out-of-synch images. Note that the accompanying out-of-synch banding is more prominent at slower disk speeds (i.e. later in the kinetic series) than earlier.

Change disk speed from 5000 to 1800 rev/min

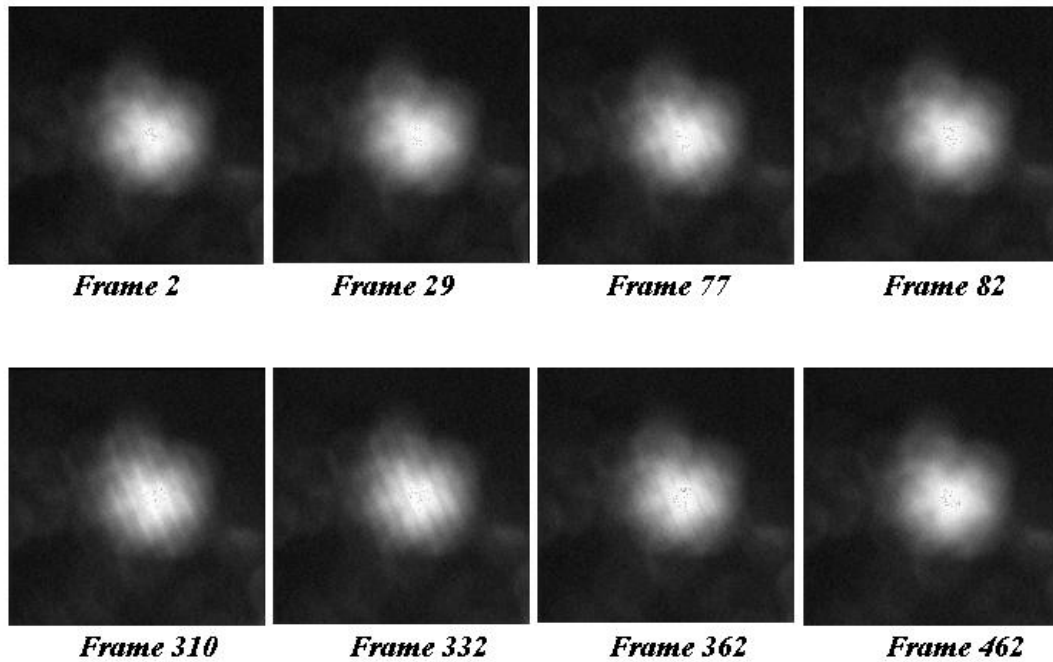


Figure 4 – Selected frames from a 500 frame kinetic series showing effect on synchronisation banding as CSU22 disk speed is changed from 5000 to 1800 rev/min. A 19.44 ms EMCCD exposure time was employed, corresponding to synchronisation with the 1800 rev/min final disk speed.

It is also interesting to record an extended kinetic series as the disk slows from a stable rotation speed to a complete stop. Figure 5 shows a montage of selected frames from a 500 frame kinetic series, following the disk from a maximum speed of 5000 rev/min to a standstill. The CCD exposure time used was 16 ms (49 frames/sec – the complete CCD cycle time under the conditions used was 20.4 ms), 16 ms corresponding to the time taken for 16 full Nipkow disk scans (16 segment passes) at 5000 rev/min. It is clear that the two are in-synch during early frames moving quickly to an out of synch superimposed band pattern as the disk begins to slow. As the disk slows further the images pass through several further cycles of this effect, the banding becoming more prominent during out-of-synch phases later in the series. The banding pattern is more prominent at slower disk speeds as the partially scanned Nipkow images represent a greater proportion of the CCD exposure time, relative to when the disk is revolving faster. Finally the disk comes to a halt revealing images of the stationary pinholes (albeit slightly out of focus).

The next step in the evaluation was to confirm that it is possible to hold the CSU22 at a fixed spin speed and then calculate a series of CCD exposure times with which it is compatible. The maximum spin speed of 5000 rev/min was chosen first of all, which corresponds to a 1000 confocal images per second. For this speed, any CCD exposure time that is a multiple of 1 ms should show synchronization and is therefore a very flexible speed to work at in terms of adapting to a large number of closely spaced CCD frame rates. The selection of CCD exposure times shown against number of incorporated Nipkow disk segments at 5000 rev/min is shown in Table 2(a). Figure 6 (a) shows selected defocused granule images taken from kinetic series of images at different exposure times for the Nipkow disk spinning at 5000 rev/min. It is clear, in accordance with the theory, that synchronisation is achieved for exposure times which are a multiple of 1 ms, whereas exposure times incorporating a fraction of a ms show a non-synchronised banding pattern. It is also evident that the banding pattern is much less prominent at longer exposure times, in line with the expectation that partial Nipkow scans represent a lesser contribution to the CCD exposure under these conditions. In this context, it is under conditions of longer CCD exposure times and fastest disk speed that the CSU22 will be most effective, even when not synchronised to the CCD exposure.

Reduce disk speed from 5000 rev/min to standstill

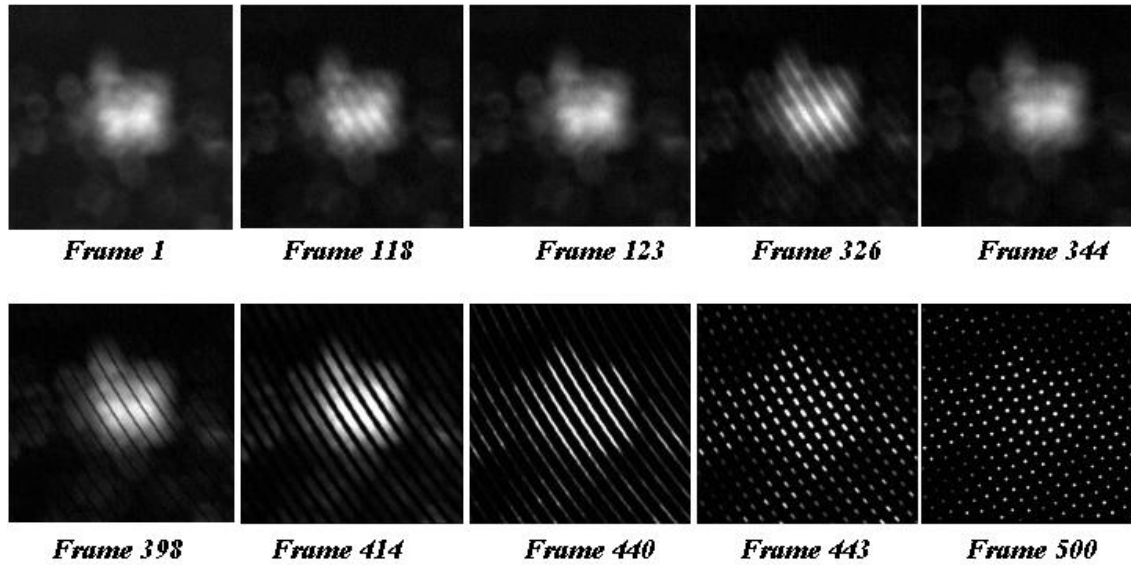


Figure 5 – Selected frames from a 500 frame kinetic series showing effect on synchronisation banding as CSU22 disk speed is changed from 5000 to a complete standstill. A 16 ms EMCCD exposure time was employed, corresponding to synchronisation with the 5000 rev/min final disk speed.

(a) – 5000 rev/min

Nipkow segments	Frame rate / Hz	CCD exposure time / ms
1	1000	1
2	500	2
3	333.33	3
4	250	4
5	200	5
6	166.67	6
7	142.86	7
8	125	8
9	111.11	9
10	100	10
11	90.91	11
12	83.33	12
13	76.92	13
14	71.43	14
15	66.67	15
16	62.5	16
17	58.82	17
18	55.55	18
19	52.63	19
20	50	20
21	47.62	21
22	45	22
23	43.48	23
24	41.67	24

(b) – 1800 rev/min

Nipkow segments	Frame rate / Hz	CCD exposure time / ms
1	360	2.78
2	180	5.55
3	120	8.33
4	90	11.11
5	72	13.89
6	60	16.66
7	51.43	19.44
8	45	22.22
9	40	25
10	36	27.78
11	32.73	30.55
12	30	33.33
13	27.69	36.11
14	25.71	38.89
15	24	41.67
16	22.5	44.44
17	21.18	47.22
18	20	50
19	18.95	52.78
20	18	55.55
21	17.14	58.33
22	16.36	61.11
23	15.65	63.89
24	15	66.67

Table 2 – Tables showing synchronisable CCD exposure times calculated for disk spin rates of (a) 5000 rev/min and (b) 1800 rev/min.

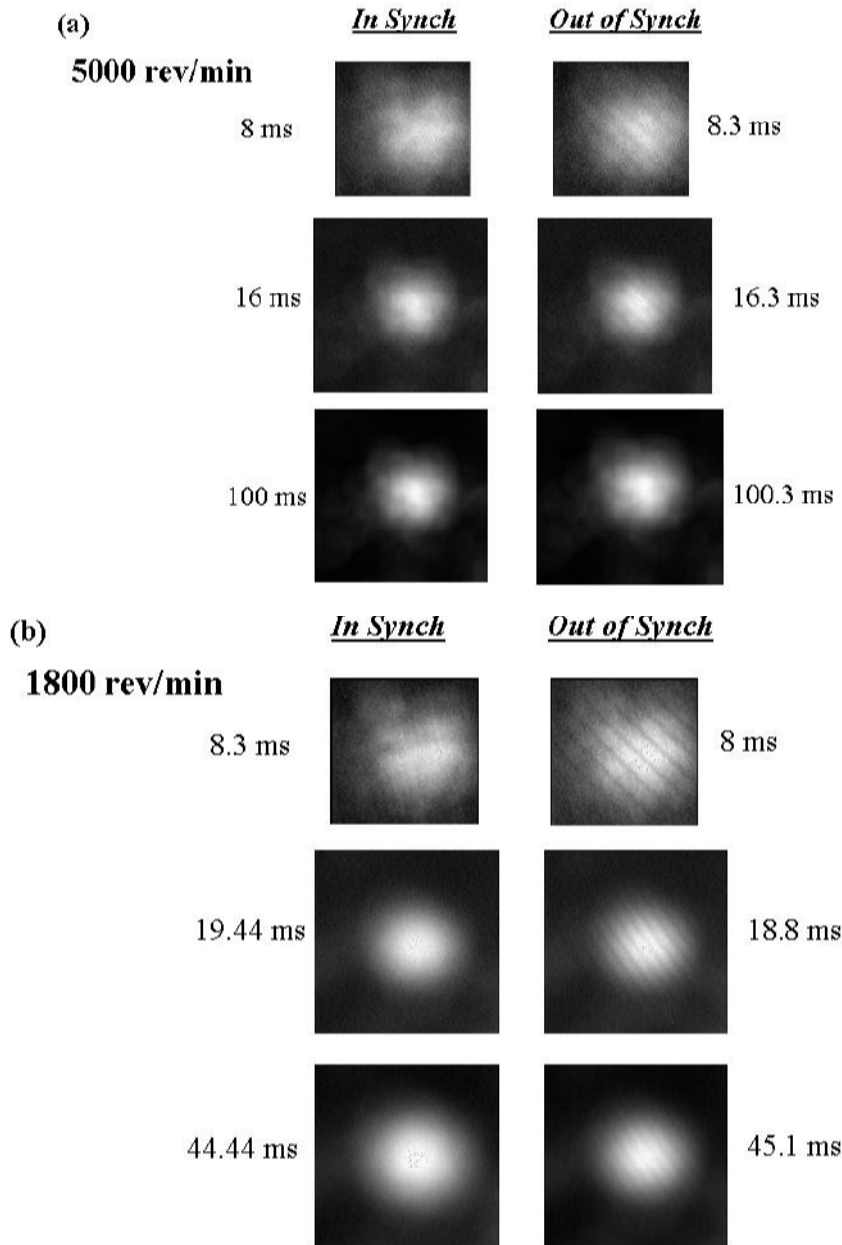


Figure 6 –Selected frames from kinetic series showing effect of exposure synchronisation to banding effect at CSU22 disk speeds of 5000 and 1800 rev/min.

It is also of interest to hold the CSU22 at 1800 rev/min, since this is the reported fixed speed for the CSU10 unit. A series of calculated exposure times that should give synchronisation at this disk speed is given in Table 2(b). Recording images at each of these exposure times did indeed result in perfectly synchronised images, the banding pattern completely deleted from each, whereas exposure times chosen between the values in the table showed the banding effect. Figure 6 (b) shows a selection of such images at a variety of synchronised and non-synchronised exposure times.

We are presently making efforts to enable the user to control the CSU22 speed through the Andor imaging software, such that the most suitable speed can be chosen to yield synchronisation with a selected camera frame rate. We are also programming a series of selectable exposure times that will give synchronisation with the fixed speed, 1800 rev/min CSU10 unit.

It is worth pointing out also that CSU units were designed to yield synchronisation with PAL and NTSC video rate cameras. However, the standard video camera has insufficient sensitivity for this technique.

C- Synchronisation of the CSU10

Since many research groups have the 1st generation CSU10 Nipkow confocal unit installed in their laboratories, it is of particular interest to verify that we can apply the methods of synchronisation to this system also. As mentioned, one of the fundamental distinctions of this version is that it operates at a fixed 1800 rev/min disk speed. Therefore, a series of CCD exposure times can be selected from which one can readily synchronise to the disk speed. This exposure time series has already been calculated and is shown in Table 2(b).

A series of ink granule images at different exposure times taken from the table were recorded (all of which have been calculated to yield synchronised images), alongside a series of exposure times that should result in non-synched images. It was again clear that the values of 11.11 ms and 22.22 ms from Table 2(b) do indeed result in clean images, whereas those values not in the table show banding patterns. However in this case, it was also apparent that the values of 8.33 ms and 19.44 ms from the table, which were expected also to represent synchronisation, instead show a defined banding pattern. In fact, upon working through the values in this 1800 rev/min table, it became apparent that only every second value of the list showed complete eradication of the banding pattern, beginning with value of 5.55ms, which would have corresponded to two of the image segments of the CSU22. It therefore seems apparent that an image of the CSU10 disk, provided it is indeed spinning at 1800 rev/min, corresponds to a segment making up one sixth of the disk area, not one twelfth. The underlying reason for this distinction is being investigated further. Irrespective of the reason though, this reduces by a factor of two the number of available synchronisable CCD exposure times across the range, however, there remains an adequate number for coverage of most experimental scenarios. It seems therefore that one of the benefits of the CSU22 is that exposure synchronisation can be considered entirely tuneable across the range of CCD exposure times, whereas the CSU10 must make do with a defined selection of synchronisable CCD exposure times across the range. Nevertheless, the CSU10 is entirely synchronisable and by a relatively simple method, a protocol that can find widespread use amongst many research groups.

It was worth confirming the presence of the frame shift effect for the CSU10 also. Using a synchronised exposure value of 22.22 μ s and a vertical shift time of 6.6 μ s/row, a 500 frame kinetic series was recorded while rotating the camera on its c-mount attachment to the Nipkow unit. As expected, the camera moved through some orientations that did not yield the frame transfer banding from the bright regions of the image. This is entirely consistent with that observed for the CSU22 unit. As before, a kinetic series was also recorded using the same exposure value but a shorter vertical shift time of 0.6 μ s/row. It is again significant that the use of shorter vertical shift has totally rectified the frame shift problem, resulting in a completely band-free series of images at all orientations.

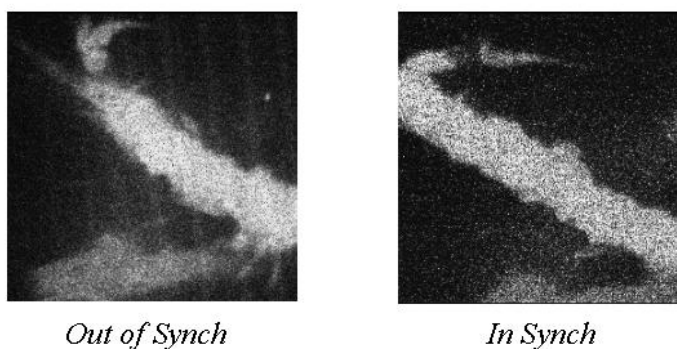


Figure 7 – Fluo-4 loaded smooth muscle cell recorded with EMCCD camera (full gain) and CSU10 spinning disk under conditions of both non-synchronisation and synchronisation; exposure time ~ 16 ms.

We also carried out some confocal experiments on smooth muscle cells loaded with Fluo-4 Ca²⁺ dye in order to demonstrate the banding patterns within these images. Whilst the non-synchronisation banding is much more obvious when viewing the images as a kinetic series playback, the band pattern can indeed be recognised from the 6.6 μ s vertical

shift, non-synchronised image in Figure 7. Choosing a near-by synchronised exposure time and a shorter vertical shift time results in a clean image.

4. CONCLUSIONS

Clear methods have been described to completely eliminate undesirable image banding patterns that are often observed when using a Nipkow spinning disk confocal microscopy equipment with a fast frame rate CCD. This has been realised through understanding of both synchronisation effects and also optimisation of the EMCCD frame transfer process. This understanding is crucial in removing one of the final barriers to widespread usage of the combined Nipkow/EMCCD technologies for rapid live cell fluorescence microscopy. Although the results here are described for synchronisation to a microlens type confocal spinning disk design, it is entirely reasonable to assume the principles will work for any such unit.

5. REFERENCES

1. P. Jerram et al, "*The LLLCCD: Low Light Imaging without the need for an Intensifier*", Proc. of SPIE, **Vol 4306**, 2001.
2. C. D. Mackay et al, "*Sub-Electron Read Noise at MHz Pixel Rates*", <http://www.marconitech.com/ccds/l3vision/technology.php>.
3. C. G. Coates, D. J. Denvir, M. A. Hollywood, N. G. McHale, K. D. Thornbury and M. A. Hollywood "*Ultra-sensitivity, Speed and Resolution: Optimising Low-light Microscopy with the Back-illuminated Electron Multiplying CCD*", Proc. of SPIE, **Vol 5139**, pp56-66, 2003.
4. D. J. Denvir and Colin G. Coates, "*Electron Multiplying CCD Technology: Application to Ultrasensitive Detection of Biomolecules*", Proc. of SPIE **Vol 4626** pp502-512, Jan 2002.
5. D. J. Denvir and Emer Conroy, "*Electron Multiplying CCD Technology: The New ICCD*", SPIE Annual Meeting, **Vol 4796**, pp164-174, July 2002.
6. G. P. Sergeant, M. A. Hollywood, K. D. McCloskey, K. D. Thornbury, and N. G. McHale, "*Specialised Pacemaking Cells in the Rabbit Urethra*", J. Physiol. **Vol 526**, pp359-366, 2000.
7. M. A. Hollywood, L. Johnston, N. G. McHale and K. D. Thornbury, "*Spontaneous Calcium Transients in Isolated Interstitial Cells from the Rabbit Urethra*", J. Physiol **Vol 548**, 2003 (in press).
8. S. Inoue and T. Inoue, "*Direct-view High-speed Confocal Scanner: The CSU-10*", Methods in Cell Biology **Vol 70**, pp87-127, 2002.
9. T. Tanaami, S. Otsuki, N. Tomosada, Y. Kosugi, M. Shimizu, H. Ishida, "*High-speed 1-Frame/ms Scanning Confocal Microscope with a Microlens and Nipkow Disks*", Applied Optics **Vol 41**, pp4704-4708, 2002.